Investigation of the Effect of Crabbing Velocity on Squeal Noise based on a Rolling Contact Two Disc Test Rig

Xiaogang Liu[1*], Paul Meehan[2]

[1]*Wuhan University of Technology, Wuhan, China*
[2]*University of Queensland, Brisbane, Australia*

e-mail: *Xiaogang_liu@yahoo.com*

ABSTRACT

The effect of crabbing velocity, namely lateral sliding velocity, on the sound pressure level of squeal noise is investigated using a rolling contact two disk test rig. The sound is recorded at various crabbing velocities when the test rig is running at different rolling speeds. The results show that the sound pressure level of squeal noise increases with crabbing velocity even though the rolling speeds are different when the sound was recorded. The vibration velocity of the test rig's lower wheel is simulated using a mathematical model in the time domain. The results show that the vibration velocity increases steadily until its amplitude approximates to the crabbing velocity. Furthermore, the lateral force and power input at different instants are simulated to illustrate the reason for this phenomenon. The research presented in this paper provides a theoretical foundation for mitigating squeal noise by controlling crabbing velocity.

1. INTRODUCTION

Railway transportation is continuing to grow due to its relative merits such as high safety, predictable punctuality and large capacity. With the ongoing increases in speed and growth in traffic intensity, one kind of railway noise, curve squeal, is becoming more prominent. Field tests found that the sound pressure level of curve squeal is normally 30 dB higher than that of normal rolling noise. Currently, it is generally agreed that curve squeal is associated with excessive lateral crabbing at the contact patch of wheel/rail interface [1]. When a bogie negotiates a curve of a track, there is a misalignment between the rolling velocity and the wheel velocity, leading to a lateral sliding velocity of the wheel across the top of rail, as shown in Fig. 1. This lateral sliding velocity between the wheel and rail is also called crabbing velocity in brief.
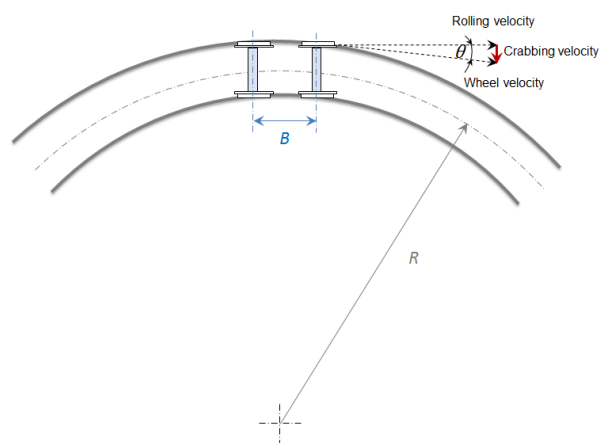
Fig. 1. The kinetics of the curve squeal generation

Many mathematical models have been developed to understand the mechanism of curve squeal but less have focused on squeal amplitude and noise level. A time domain model was presented by Heckl and Abrahams [2], which focused on the squeal noise generated by a flat round disc excited at one point along the edge by a dry-friction force dependent on the

disc velocity. This paper concluded that curve squeal is an unstable wheel oscillation that grows to a limit cycle oscillation, whose velocity amplitude is equal or very close to the crabbing velocity. Furthermore, the simulation results of Chiello et al. [3] also showed that the vibration velocity stabilises below the lateral sliding velocity. The detailed explanation for these phenomena, however, has not been provided yet.

2. METHODOLOGIES

The experiments in this paper are based on a rolling contact two disc test rig developed for the investigation of squeal noise. A theoretical model in the time domain is used for further investigation and illustration. The parameters used for numerical simulation are also derived from the characteristics of this test rig.

2.1 Experimental methods

A rolling contact two disc test rig is used to investigate the effect of crabbing velocity on squeal noise as demonstrated in Fig. 2 (a).

(a)

(b)
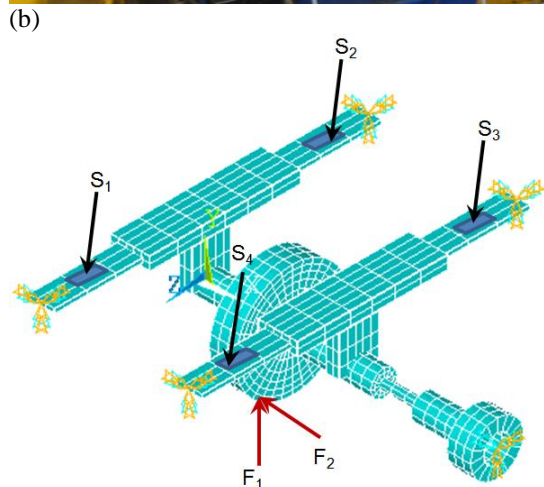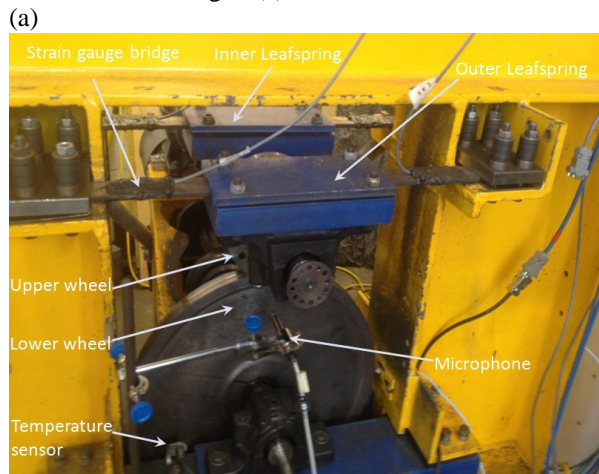
Fig. 2. Rolling contact two disc test rig used for the investigation of sqeual noise (a) front view of the test rig, (b) the FEM model of the test rig structure [4]

The lateral force between the upper and lower wheel can be measured with strain gauge bridges as marked in Fig. 2 (b) and this method has been introduced in details in [4]. Some parameters of this test rig are listed in Table 1.

Table 1. Parameters of the test rig [5]

Description	Value
Radii of longitudinal and tangential curvature for the lower wheel (R_1, R_{1t})	0.213 m, 0.300 m
Thickness of the lower wheel (rim, web)	0.026 m, 0.015 m
Density (ρ)	7800 kg/m^3
Inner radius of lower wheel (R_1')	0.0325 m
Young's modulus of upper and lower wheel (E)	175 GPa
Radii of longitudinal and tangential curvature for the upper wheel (R_2, R_{2t})	0.085 m, 0.040 m
Thickness of the upper wheel	0.080 m
Poisson's ratio (v)	0.28
Angle of attack range	0 ~ 26 mrad
Creep coefficient (C_{22})	3.14
Normal loading (W)	1000 N
Modal mass (m)	3.1 kg
Modal damping (c)	42 Ns/m
Modal stiffness (k)	1.6E8 N/m

The angle of attack between the upper and lower wheel can be adjusted and measured using the method introduced in [6]. The test rig was run at various crabbing velocities and the sound was recorded with a microphone placed 0.05 m away from the lower wheel and 0.8 m above the ground as displayed in Fig. 2 (a). The vibration characteristics of the test rig are investigated with modal tests conducted with a hard tip impact hammer and analysed using the finite element method. The vibration characteristics of the lower wheel acquired from finite element analysis and modal tests correlate well with the results of sound recording [5]. Therefore, the investigation of the effect of crabbing velocity on wheel vibration can indicate its effect on squeal noise.

2.2 Theoretical modelling

A 1-DOF model was developed in a previous paper [6], and it is used in this research further to illustrate the effect of crabbing velocity on squeal noise. As described in Fig. 1, the crabbing velocity is due to the misalignment between the wheel velocity and rolling velocity. The lateral force Q at the contact point should be opposite to the direction of crabbing velocity V_c as marked in Fig. 3 (a). In the lateral direction, the dominant vibration of the wheel is analogue to the friction self-excited oscillation of mass connected to a spring and damping on a rolling belt as demonstrated in Fig. 3 (b).

(a)
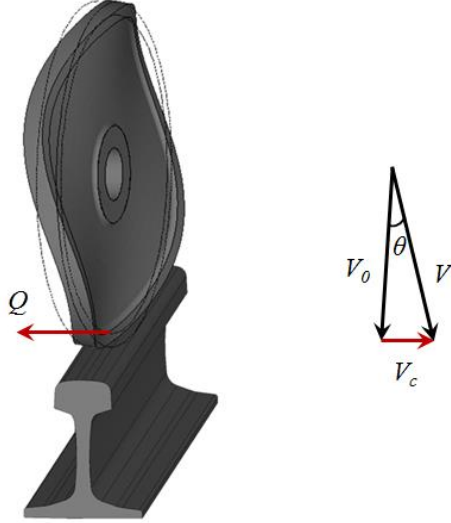
(b)
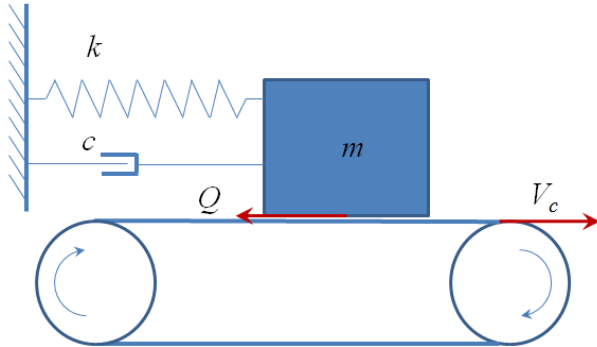
Fig. 3. (a) 3D demonstration of a wheel rolling on rail top, (b) 1-DOF friction self-excited oscillation in lateral direction

The wheel vibration can be described with the motion of a spring-mass-damper system that can be expressed as,

$$m\ddot{y}(t) + c\dot{y}(t) + ky(t) = Q(\zeta) \tag{1}$$

where m is the modal mass, c is the damping coefficient, k is the modal stiffness. The modal parameters of the dominant mode were curve fitted from the receptance spectrum of the modal test and listed in Table 1. The lateral force Q can be calculated with,

$$Q = -\mu(\zeta)W \tag{2}$$

Where the creepage dependent lateral adhesion ratio in rolling contact $\mu(\zeta)$ can be acquired with Equation (3).

$$\mu(\zeta) = \begin{cases} \mu_s\{\zeta' - \dfrac{1}{3}\zeta'^2 + \dfrac{1}{27}\zeta'^3\}\{1 - 0.5e^{-0.138/|\zeta V_0|} - 0.5e^{-6.9/|\zeta V_0|}\} & for\ \zeta' \le 3 \\ \mu_s\{1 - 0.5e^{-0.138/|\zeta V_0|} - 0.5e^{-6.9/|\zeta V_0|}\} & for\ \zeta' > 3 \end{cases} \tag{3}$$

where μ_0 is the stationary friction coefficient, the lateral creepage ζ is the ratio of the lateral relative velocity between the wheel and rail divided by rolling speed V_0 [7].

$$\zeta = (V_c + \dot{y}(t))/V_0 \tag{4}$$

where $\dot{y}(t)$ is the vibration velocity of the wheel, V_c is crabbing velocity. The lateral crabbing velocity between two wheels can be calculated with angle of attack θ and rolling speed V_0, i.e., $V_c = V_0 sin\ \theta$. As the angle of attack is normally less than 3 degree, the crabbing velocity can be described with,

$$V_c = \theta V_0 \tag{5}$$

The ζ' in Equation (3) is a normalised creepage that can be described with,

$$\zeta' = \frac{\zeta GabC_{22}}{\mu_0 W} \tag{6}$$

where $G = E/2(1+\upsilon)$. The values used for elastic modulus E, Poisson's ratio υ, the constant C_{22} and the normal loading W are listed in Table 1. The dimensions of elliptical contact patch, a and b, are determined by the contact theory of Hertz [8].

When the effect of viscous damping is considered, the power input due to the lateral force and damping dissipation can be expressed as,

$$P_{Qd} = Q\dot{y}(t) - c(\dot{y}(t))^2 \tag{7}$$

where c is the modal damping of the dominant mode listed in Table 1.

3. RESULTS AND DISCUSSIONS

Firstly, the results about the effect of crabbing velocity on squeal noise are presented. Furthermore, the effect of crabbing velocity on wheel vibration is simulated and analysed.

3.1 Experimental results based on the rolling contact two disc test rig

The rolling contact two disc test rig was set at various angles of attack, from 0 to 26 mrad. For each yaw angle the test rig was run at the rolling speeds of 400 RPM, 600 RPM and 800 RPM (the corresponding linear velocity at the contact point are 8.9, 13.4 and 17.8 m/s, respectively). The lateral adhesion ratio was measured with strain gauge bridges. In particular, the results measured at 800 RPM are presented in Fig. 4.

The measured results can show a nonlinear friction creepage relationship as observed by Remington [9], which is based on lateral creep data from a roller rig. Furthermore, the friction creepage relationship is simulated via the model introduced previously. Both experimental measurements and numerical simulation indicate the nonlinear relationship between the friction and creepage.
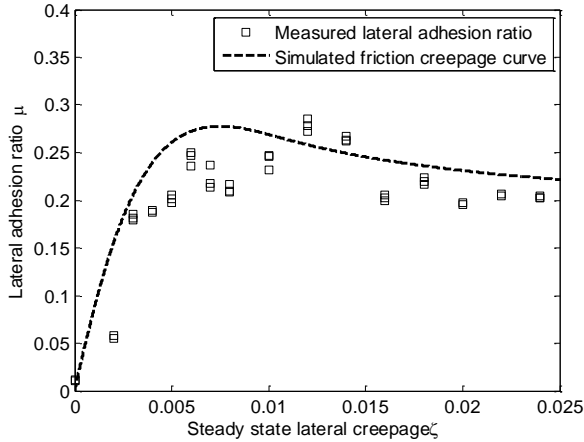
Fig. 4. Experimental measurements and simulated friction-creep curves at 800 RPM

The sound generated by the rolling contact two disc test rig was recorded with a microphone and the recorded sound data is analysed and presented in Fig. 5.
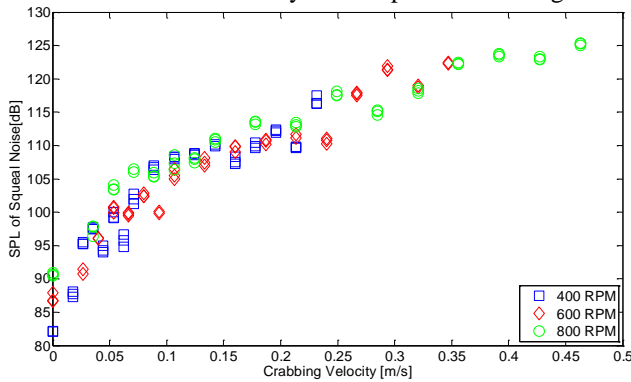
Fig. 5. The sound pressure level of squeal noise versus crabbing velocity

The experimental results in Fig. 5 show that the sound pressure level (SPL) of squeal noise increases with crabbing velocity. The noise level is higher for 800 RPM when the crabbing velocity is zero, because the recoded sound is mainly rolling noise, which is more relevant to rolling speed. With the increase of crabbing velocity, however, squeal noise become the dominant part of the sound and the effect of crabbing velocity on the sound pressure level of squeal noise turns to be dominant and evident. Therefore, it can be observed in Fig. 5 that the sound pressure levels of squeal noise acquired at different rolling speeds correlate well with each other when the crabbing velocity is larger than 0.1 m/s.

3.2 Theoretical analyses based on the mathematical model

To illustrate the effect of crabbing velocity on wheel squeal, the vibration of the wheel is simulated at the rolling speed of 800 RPM and the crabbing velocity of 0.39 m/s, using the theoretical model in the time domain. The simulated results show that the vibration velocity amplitude keeps increasing, until it is stabilised at a certain value, which is marginally less than the corresponding crabbing velocity as presented in Fig. 6. For this case, the quasistatic lateral creepage is 0.022, which equals to the value of angle of attack between the lower and upper wheel. Fig. 6 shows that when the initial vibration velocity is 0 m/s and the displacement is 0 m, the vibration velocity increases steadily until it reaches a limited cycle oscillation whose amplitude approximates to the crabbing velocity.
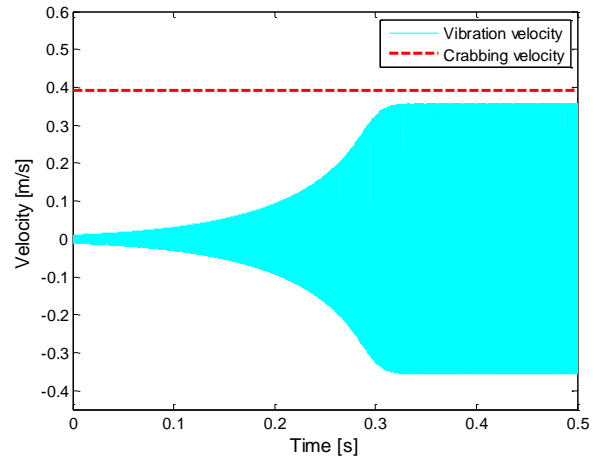
Fig. 6. The simulated vibration velocity at certain crabbing velocity

In particular, the vibration velocity and its corresponding lateral force around 0.2 s can be simulated as demonstrated in Fig. 7 (a). In the mathematic model, Equation (3) indicates that the lateral adhesion ratio in rolling contact is determined by the lateral creepage, while Equation (4) indicates the lateral creepage is determined by crabbing velocity and vibration velocity. Therefore, the variation of the corresponding lateral force is also simulated as presented in Fig. 7 (b).

(a)

(b)
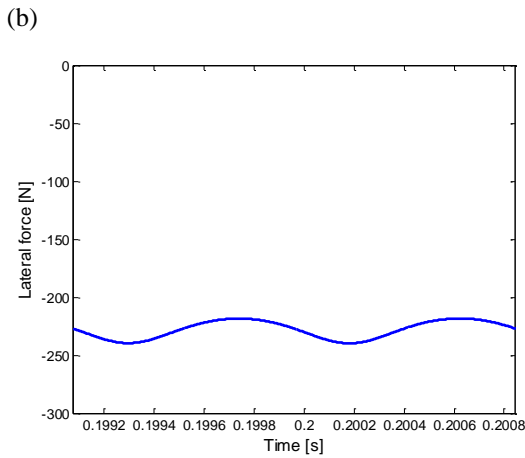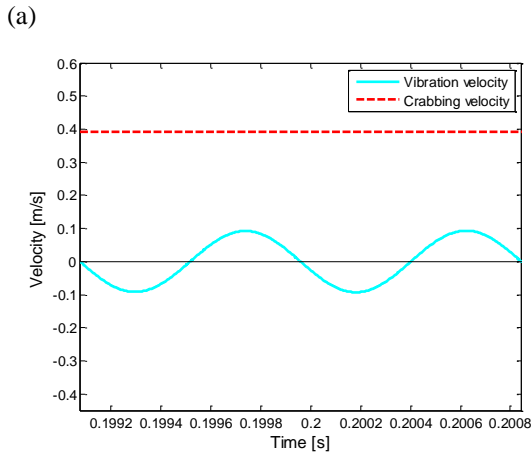
Fig. 7. Simulated vibration velocity (a) and the corresponding lateral force (b) around the time of 0.2 s

The corresponding power input can be acquired according to Equation (7) as demonstrated in Fig. 8. The result shows that the vibration system gains power input in the oscillation cycle around the time of 0.2 s. Specifically, when the lateral force is in the same direction with the vibration velocity, it adds dynamic energy into the vibration system. Otherwise, the lateral force consumes dynamic energy from the vibration system when the vibration velocity is in the opposite direction with the lateral force. At the instant of 0.2 s, the lateral force adds more dynamic energy when it is in the same direction with the vibration velocity than the consumed energy when it is in the opposite direction with the vibration velocity.
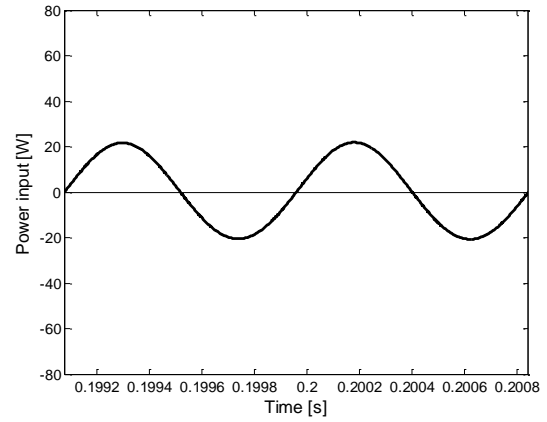
Fig. 8. The power input around the time of 0.2 s

In contrast, the vibration velocity and its corresponding lateral force around 0.4 s can be simulated as demonstrated in Fig. 9 (a) and (b), respectively.

(a)

(b)
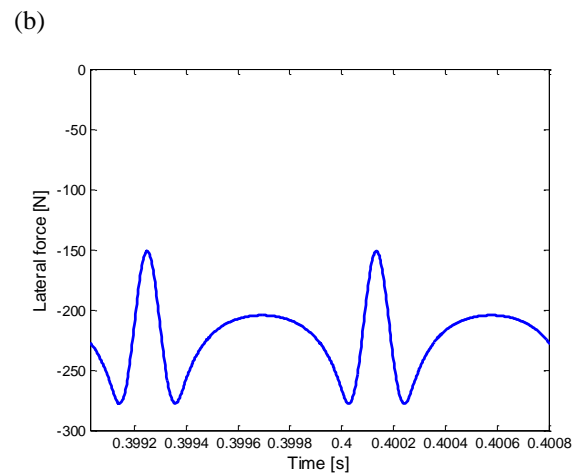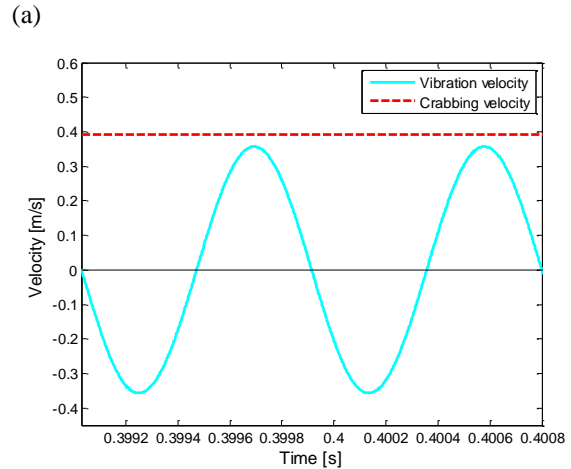
Fig. 9. Simulated vibration velocity (a) and the corresponding lateral force (b) around the time of 0.4 s

Fig. 9 (a) shows that the vibration velocity amplitude approximates to the crabbing velocity around the time of 0.4s. The nonlinear friction creepage interacts with the wheel vibration as described in Equation (4). According to the friction-creepage relationship described in Equation (3), the lateral force starts to

decrease when the lateral creepage range passed the critical creepage around 0.008 in Fig. 4. Therefore, the lateral force fluctuates dramatically as demonstrated in Fig. 9 (b). Furthermore, the corresponding power input can be acquired according to Equation (7) as demonstrated in Fig. 10.
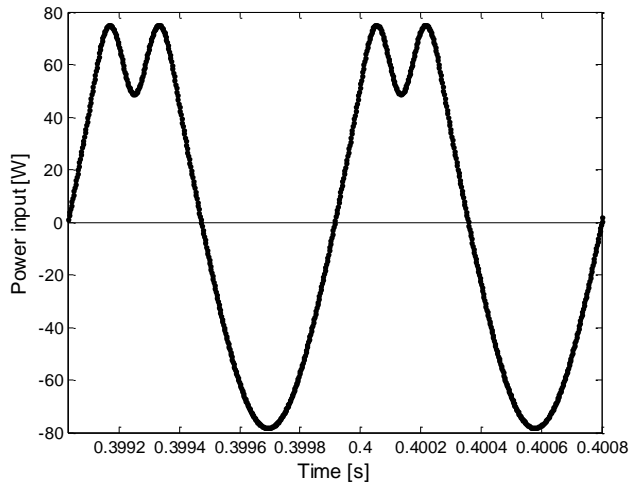
Fig. 10. The power input around the time of 0.4 s

The gaps in the power input in Fig. 10 are due to the sudden reductions of lateral force in Fig. 9 (b). Comparing Fig. 9 (a) and (b), one can notice that the lowest lateral force corresponds to the highest vibration velocity that is in the same direction with the lateral force. The result shows that the vibration system gains no more energy input in these oscillation cycles around 0.4 s, when the vibration velocity approaches the crabbing velocity. The reason why the vibration velocity stabilised at a value close to the crabbing velocity is that the dynamic energy input from the lateral force is no more than the energy consumption from the lateral force anymore when the vibration velocity amplitude approximates to the crabbing velocity. As a result, the sound pressure level of squeal noise increases with the crabbing velocity. Therefore, it seems that the squeal noise can be mitigated if the crabbing velocity can be controlled.

4. CONCLUSIONS

A rolling contact two disk test rig is used to investigate the effect of crabbing velocity on the sound pressure level of squeal noise. The test rig is run at various crabbing velocity at the rolling speed of 800, 600 and 400 RPM. The results show that the sound pressure level of squeal noise increases with crabbing velocity. In particular, the results derived from the sound recorded at different rolling speeds also correlate well with one another.

A mathematical model in the time domain integrating the contact mechanics with the vibration of the wheel is used to simulate the vibration velocity of the test rig's lower wheel. The results show that the vibration

velocity increases steadily until its amplitude approaching to the crabbing velocity approximately. Furthermore, the reason for this phenomenon is investigated via the theoretical model. The lateral force and power input at the instants when the vibration amplitude is still growing and when the amplitude approaches a stable value approximated to the crabbing velocity are simulated. The results show that the reason why the vibration velocity amplitude stabilises at a value close to the crabbing velocity is that the energy input reaches a balance when the vibration velocity approximates to the crabbing velocity.

The discovery of the effect of crabbing velocity on the sound pressure level of squeal noise provides a theoretical foundation of curbing squeal noise via reducing crabbing velocity between the wheel and rail. Promisingly, some more practical mitigation methods for squeal noise might be developed based on the research presented in this paper.

5. REFERENCES

[1] M.J. Rudd, Wheel/rail noise--Part II: Wheel squeal, Journal of Sound and Vibration, 46 (1976) 381-394.
[2] M.A. Heckl, I.D. Abrahams, Curve squeal of train wheels, part 1: Mathematical model for its generation, Journal of Sound and Vibration, 229 (2000) 669-693.
[3] O. Chiello, J.B. Ayasse, N. Vincent, J.R. Koch, Curve squeal of urban rolling stock--Part 3: Theoretical model, Journal of Sound and Vibration, 293 (2006) 710-727.
[4] X. Liu, P.A. Meehan, Investigation of the effect of relative humidity on lateral force in rolling contact and curve squeal, Wear, 310 (2014) 12-19.
[5] X. Liu, P.A. Meehan, Wheel squeal noise: A simplified model to simulate the effect of rolling speed and angle of attack, Journal of Sound and Vibration, 338 (2015) 184-198.
[6] X. Liu, P.A. Meehan, Investigation of the effect of lateral adhesion and rolling speed on wheel squeal noise, Proceedings of the Institution of Mechanical Engineers Part F-Journal of Rail and Rapid Transit, 227 (2013) 469-480.
[7] H. Wu, N. Wilson, Railway Vehicle Derailment and Prevention, in: Handbook of Railway Vehicle Dynamics, CRC Press, 2006.
[8] K.L. Johnson, Contact Mechanics, cambridge university press, London, 1985.
[9] P.J. Remington, Wheel/rail squeal and impact noise: What do we know? What don't we know? Where do we go from here?, Journal of Sound and Vibration, 116 (1987) 339-353.